

AMPOSE: ALTERNATIVELY MIXED GLOBAL-LOCAL ATTENTION MODEL FOR 3D HUMAN POSE ESTIMATION

Hongxin Lin, Yunwei Chiu and Peiyuan Wu

National Taiwan University, Taiwan

ABSTRACT

The graph convolutional network (GCN) has been applied to 3D human pose estimation (HPE). In addition, the pure transformer model recently shows promising results in the video-based method. However, the single-frame method still needs to model the physically connected relations among joints because the feature representation transformed only by global attention lack the relationships of the human skeleton. To deal with this problem, we propose a novel architecture, namely AMPose, to combine the physically connected and global relations among joints in the human skeleton towards human pose estimation.

The effectiveness of our proposed method is demonstrated through evaluation on Human3.6M dataset. Our model also shows better generalization ability by cross-dataset comparison on MPI-INF-3DHP. Code can be retrieved at <https://github.com/erikervalid/AMPose>.

Index Terms— GCNs, Transformer, 3D human pose estimation, 2D-3D lifting

1. INTRODUCTION

Human pose estimation (HPE) is attractive to researchers in computer vision. Particularly, 3D HPE is rather related to real-world applications in human-robot interaction, rehabilitation, and augmented reality. Most previous works built their model via the 2D-3D lifting method, which inferences the 2D keypoints in images by off-the-shelf 2D pose models firstly [1, 2, 3], and then the 2D keypoints are taken as the input of lifting models to predict 3D keypoints. The method of separating 3D HPE into two phases can abate the influence of image background [2].

3D HPE in the video has been developed for several years [2, 4, 5]. Temporal modeling usually regards temporal information as independent dimension of data or tokens, which demands performance computing to run these models [4, 5]. Considering the computational cost, single-frame models can be easier for real-world applications.

Some works have shown that feature transformed from 2D keypoints can be useful information to estimate 3D positions [2]. To solve the lack of capturing the spatial relationships

among joints, graph convolutional networks (GCNs) have recently been adopted in many HPE models [3, 6, 7, 8]. A drawback of the vanilla GCNs derived from spectrum convolution is weight-sharing convolution. Each node in vanilla GCNs is transformed by the same transformation matrix, and then the neighboring features will be aggregated to transfer the information to next layer [9]. The weight-sharing method may not work well to capture the information of human articulation because the flexibility and speed of human motion can vary with joints [3].

Non-local dependency among joints in 3D HPE remains unclear. The Transformer-based models in computer vision have recently shown high performance in various tasks [10, 5]. The self-attention used in Transformer can capture the global information of the features [5]. In the case of 3D HPE, the self-attention can make the joints relate to the other joints to obtain global dependency. The self-attention is suitable to model the similarity relations among joints since the global dependence can alter with the different input pose [1, 4]. In spite of that, pure transformer models may result in lacking the physical information in the human skeleton [1].

To fully exploit the local and non-local relations among joints in the human skeleton, we proposed a novel architecture that can alternatively mix the information of local and global dependency by two independent modules, which are the GCN block and Transformer encoder, respectively.

Contributions in this paper can be summarized as follows: 1) A novel structure AMPose is proposed to independently capture global and local information in the human skeleton. 2) Different designs are explored for the graph convolution block, which improves the performance of graph convolution and fully exploits the physical-connectivity feature. 3) Our model outperforms the state-of-the-art model on the Human3.6M dataset. The proposed model also shows better generalization ability on MPI-INF-3DHP as compared to previous works.

2. METHODOLOGY

2.1. Overview

The overall structure of the AMPose is illustrated in Fig. 1. We aim to predict the 3D joint position. Our method takes 2D

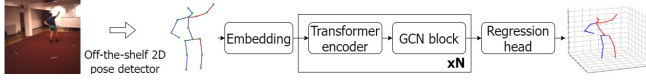


Fig. 1. Overview of the AMPose network structure.

joint positions estimated by 2D pose models first. In the proposed model, each joint pose will be transformed by a trainable linear projection layer, and then we alternatively stack the Transformer encoder and the GCN block to transform the embedding features. The feature from the last GCN block is regressed to generate the 3D pose with a linear projection layer.

2.2. Transformer encoder

Scaled Dot-Product Attention is defined as a self-attention function. This function takes query Q , key K and value V as input where $Q, K, V \in R^{N_j \times N_d}$, N_j is the number of joints and N_d is the number of channel. To prevent the extremely big product of the query and the key, $\sqrt{N_d}$ is applied for normalization. Self-attention can be formulated as follows:

$$\text{Attention}(Q, K, V) = \text{Softmax}\left(\frac{QK^T}{\sqrt{N_d}}\right)V \quad (1)$$

After the input feature $Z \in R^{N_j \times N_d}$ is transformed via learnable transformation matrix $W^Q, W^K, W^V \in R^{N_d \times N_d}$, the query, key, and value can be obtained, namely

$$Q = ZW^Q, K = ZW^K, V = ZW^V \quad (2)$$

Multi-head Self Attention Layer (MSA) is the concatenation of multiple self-attention functions. Each head partially takes the feature as input. The concatenation of multiple heads will be transformed by W^{out} . The MSA can be represented as follows:

$$\text{MSA}(Q, K, V) = \text{concat}(\text{head}_1, \dots, \text{head}_{N_h})W^{out} \quad (3)$$

where $\text{head}_i = \text{Attention}(Q_i, K_i, V_i)$, $i \in [1, \dots, N_h]$, and $W^{out} \in R^{N_d \times N_d}$ is the trainable parameter matrix.

Multi-layer perceptron (MLP) is used to project the feature of each joint with the fully connected layer (FC). The Gelu [11] is used as an activation function between FCs. The MLP can be expressed as follows:

$$\text{MLP}(z) = \text{FC}(\sigma_{\text{Gelu}}(\text{FC}(z))) \quad (4)$$

The overall process can be formulated as follows:

$$Z' = Z_0 + W_{pos} \quad (5)$$

$$Z'' = \text{MSA}(\text{LN}(Z')) + Z' \quad (6)$$

$$Z_1 = \text{MLP}(\text{LN}(Z'')) + Z'' \quad (7)$$

where Z_0 denotes the feature from the last layer, $\text{LN}(\cdot)$ represents layer normalization, W_{pos} is the positional embedding, and Z_1 denotes the output of the encoder.

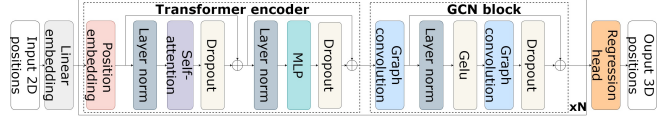


Fig. 2. An instantiation of the AMPose for 3D HPE.

2.3. GCN blocks

In these blocks, a spectral graph convolution [15, 9] is used to model the physical relations in the human skeleton since it can incorporate the information of structure data with a hand-crafted graph [3, 6]. The Chebnet [15] derived from spectral graph convolution is a k -th order polynomial on adjacency matrix. The high-order polynomial results in overfitting and higher computational complexity [15]. Thus Kipf *et al.* [9] simplify the spectral graph convolution with the first-order approximation, which also shortens the receptive field of the filter to the 1-hop range. The formula of the vanilla GCN is as follows:

$$Z = D^{-0.5}AD^{-0.5}X\Theta \quad (8)$$

Where $A \in \{0, 1\}^{N_j \times N_j}$ denote the adjacency matrix which includes the self-loop edges for all nodes, the diagonal matrix $D \in R^{N_j \times N_j}$ is the degree matrix of A , $X \in R^{N_j \times N_d}$ is the signal, $\Theta \in R^{N_d \times N_D}$ is filter parameters, $Z \in R^{N_j \times N_D}$ is the output signal, N_j is the number of nodes in the graph, N_d is the input dimension of the signal, and N_D is the output dimension of the signal.

The vanilla GCNs are originally proposed to address the node classification problem. The fully weight-sharing operation can be used to solve the classification problem, but the HPE comprehends complex human motion and different flexibility for each joint. Prior works [16, 3] proposed to describe semantic relations among joints with more parameters to solve these problems. In our work, we adopt the similar design method as ST-GCN [3], but we only classify the joint nodes into three groups based on the idea of physical and local relationships in the human skeleton: 1) The center joint itself. 2) Neighboring joints which have a less number of hops to the hip than the center joint. 3) Neighboring joints which have a higher number of hops to the hip than the center joint.

The formula of graph convolution is modified accordingly: The different feature transformations are applied to different joints according to the three groups, and then the transformed feature will be aggregated, namely

$$Z = \sum_j D_j^{-0.5}A_jD_j^{-0.5}X\Theta_j \quad (9)$$

where j denotes the index of different groups, the adjacent matrix $A \in \{0, 1\}^{N_j \times N_j}$ is divided into three sub-matrices $A_j \in \{0, 1\}^{N_j \times N_j}$ according to the node group which satisfy $A_1 + A_2 + A_3 = A$, the diagonal matrix $D_j \in R^{N_j \times N_j}$ is the

Table 1. MPJPE results of various actions in millimeters on Human3.6M. Top table: 2D detector CPN with 17 keypoints used as input. Bottom table: Ground truth 2D (GT) with 17 keypoints used as input.

CPN	Dire.	Discu.	Eat	Greet	Phone	Photo	Pose	Purchu.	Sit	SitD.	Smoke	Wait	WalkD.	Walk	WalkT.	Avg.
Ci <i>et al.</i> [12]	46.8	52.3	44.7	50.4	52.9	68.9	49.6	46.4	60.2	78.9	51.2	50.0	54.8	40.4	43.3	52.7
Cai <i>et al.</i> (refinement) [3]	46.5	48.8	47.6	50.9	52.9	61.3	48.3	45.8	59.2	64.4	51.2	48.4	53.5	39.2	41.2	50.6
Pavllo <i>et al.</i> [2]	47.1	50.6	49.0	51.8	53.6	61.4	49.4	47.4	59.3	67.4	52.4	49.5	55.3	39.5	42.7	51.8
Zou <i>et al.</i> (refinement) [8]	45.4	49.2	45.7	49.4	50.4	58.2	47.9	46.0	57.5	63.0	49.7	46.6	52.2	38.9	40.8	49.4
Lutz <i>et al.</i> [13]	45.0	48.8	46.6	49.4	53.2	60.1	47.0	46.7	59.6	67.1	51.2	47.1	53.8	39.4	42.4	50.5
Ours	44.9	49.3	45.2	48.8	51.3	58.6	47.8	44.8	57.1	66.5	49.9	46.4	52.9	39.0	40.6	49.5
Ours (refinement)	42.8	48.6	45.1	48.0	51.0	56.5	46.2	44.9	56.5	63.9	49.6	46.2	50.5	37.9	39.5	48.5
GT	Dire.	Discu.	Eat	Greet	Phone	Photo	Pose	Purchu.	Sit	SitD.	Smoke	Wait	WalkD.	Walk	WalkT.	Avg.
Ci <i>et al.</i> [12]	36.3	38.8	29.7	37.8	34.6	42.5	39.8	32.5	36.2	39.5	34.4	38.4	38.2	31.3	34.2	36.3
Lutz <i>et al.</i> [13]	31.0	36.6	30.2	33.4	33.5	39.0	37.1	31.3	37.1	40.1	33.8	33.5	35.0	28.7	29.1	34.0
Zeng <i>et al.</i> [14]	32.9	34.5	27.6	31.7	33.5	42.5	35.1	29.5	38.9	45.9	33.3	34.9	34.4	26.5	27.1	33.9
Ours	30.7	35.9	30.0	33.2	33.9	37.7	37.1	31.9	34.3	41.8	33.2	34.5	34.3	27.5	28.5	33.7

degree matrix of A_j , and Θ_j is the filter parameters for the j -th group.

2.4. Loss function

To predict the 3D position with the AMPose, the mean square error is used as the loss function of our model:

$$Loss = \frac{1}{N} \sum_{i=1}^N \left\| \mathbf{X}_i - \tilde{\mathbf{X}}_i \right\|^2 \quad (10)$$

where N is the number of the human joints, i represents the index of joint type, X_i denotes the 3D ground truth positions, and \tilde{X}_i denotes the predicted 3D positions.

3. EXPERIMENTS

3.1. Dataset

The AMPose is tested on two public datasets: Human3.6M [17] and MPI-INF-3DHP [18].

Human3.6M is one among the most common datasets for 3D HPE, which is composed of 3.6 million images. The images are taken from 4 cameras arranged at different angles. Following previous work [19, 1], the 2D joint positions are normalized as the input of the AMPose. The mid hip is adopted as the root joint of the 3D pose, which localizes the 3D human positions. The AMPose is trained with subjects S1, S5, S6, S7, and S8, while tested on subjects S9 and S11.

MPI-INF-3DHP is a challenging dataset due to its various conditions. The dataset is composed of images with indoor and outdoor backgrounds along with complex and rare actions. Following prior work [19, 13], we evaluate the generalization ability of the AMPose by training on Human3.6M and testing on the test set of MPI-INF-3DHP.

3.2. Evaluation protocol

The mean per joint position error (MPJPE) is used as the evaluation protocol. MPJPE is computed as the mean of Eu-

clidean distance between the estimated 3D positions and the ground truth positions.

For cross-dataset comparison, two metrics are used to gauge the generalization ability of the proposed model: the Percentage of Correct Keypoints (PCK) and Area Under the Curve (AUC). The estimated 3D pose is regarded as the correct pose if MPJPE is below the predefined threshold. Following prior works [8, 7, 6], the threshold is set as 150 mm.

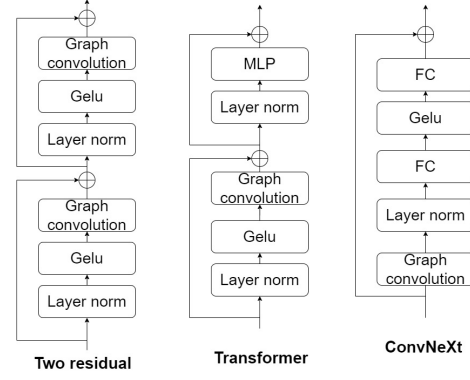


Fig. 3. Various designs for the GCN block.

3.3. Implementation details

The AMPose is built on the two-phase method. The images are first fed into the off-the-shelf 2D pose model, which is the cascaded pyramid network (CPN) [20] for our experiments on Human3.6M, and then the AMPose takes the 2D joint pose as input to generate 3D pose.

In our experiments, the depth N of the proposed model is set to 5. The number of embedding channels is set to 512. The model is trained for 50 epochs. The batch size is set to 128. The learning rate is initially set to 0.000025 along with the Adam optimizer. The learning rate decays exponentially with a factor of 0.98 for each epoch. All experiments are run on a

Table 2. MPJPE results of various actions in millimeters on Human3.6M. Top table: CPN with 16 keypoints used as input. Bottom table: GT with 16 keypoints used as input.

CPN	Direc.	Discu.	Eat	Greet	Phone	Photo	Pose	Purchu.	Sit	SitDo.	Smoke	Wait	WalkDo.	Walk	WalkTo.	Avg.
Liu <i>et al.</i> [7]	46.3	52.2	47.3	50.7	55.5	67.1	49.2	46.0	60.4	71.1	51.5	50.1	54.5	40.3	43.7	52.4
Xu <i>et al.</i> [6]	45.2	49.9	47.5	50.9	54.9	66.1	48.5	46.3	59.7	71.5	51.4	48.6	53.9	39.9	44.1	51.9
Zhao <i>et al.</i> [1]	45.2	50.8	48.0	50.0	54.9	65.0	48.0	47.1	60.2	70.0	51.6	48.7	54.1	39.7	43.1	51.8
Ours	45.8	49.1	47.8	50.0	52.9	59.0	46.9	45.8	58.9	68.0	51.1	47.2	53.6	39.9	41.8	50.5
GT	Direc.	Discu.	Eat	Greet	Phone	Photo	Pose	Purchu.	Sit	SitDo.	Smoke	Wait	WalkDo.	Walk	WalkTo.	Avg.
Liu <i>et al.</i> [7]	36.8	40.3	33.0	36.3	37.5	45.0	39.7	34.9	40.3	47.7	37.4	38.5	38.6	29.6	32.0	37.8
Xu <i>et al.</i> [6]	35.8	38.1	31.0	35.3	35.8	43.2	37.3	31.7	38.4	45.5	35.4	36.7	36.8	27.9	30.7	35.8
Zhao <i>et al.</i> [1]	32.0	38.0	30.4	34.4	34.7	43.3	35.2	31.4	38.0	46.2	34.2	35.7	36.1	27.4	30.6	35.2
Ours	31.3	36.7	30.0	34.3	34.0	37.8	38.2	32.0	36.0	40.7	34.1	34.4	34.6	28.2	29.8	34.1

Table 3. Cross dataset generalization performance comparison tested on MPI-INF-3DHP.

Method	GS	noGS	Outdoor	Avg.	PCK	AUC
Ci <i>et al.</i> [12]	74.8	70.8	77.3	74.0	36.7	
Zhao <i>et al.</i> [1]	80.1	77.9	74.1	79.0	43.8	
Liu <i>et al.</i> [7]	77.6	80.5	80.1	79.3	47.6	
Xu <i>et al.</i> [6]	81.5	81.7	75.2	80.1	45.8	
Zou <i>et al.</i> [8]	86.4	86.0	85.7	86.1	53.7	
Ours	86.1	87.5	87.4	87.0	55.2	

Table 4. The result of the different designs for the GCN block.

Method	Param. (M)	FLOPs (M)	MPJPE (mm)	Δ
Two residual	18.5	312.2	50.1	0.6
Transformer	17.0	289.8	50.1	0.6
ConvNeXt	17.0	289.9	50.0	0.5
Ours	18.3	312.2	49.5	-

machine equipped with a single NVIDIA RTX 2080 GPU.

3.4. Comparison with the state-of-the-art

Table 1 and Table 2 compare AMPose with state-of-the-art single-frame models over CPN and ground truth keypoints on Human3.6M dataset. Though some models additionally apply the pose refinement module [3] to improve the accuracy, we report the result before the refinement for fair comparisons. As shown in Table 1 and Table 2, AMPose outperforms all prior methods. Table 3 compares the generalization ability by testing the model trained on Human3.6M with MPI-INF-3DHP. We separately report the result with different backgrounds, including green screen (GS), noGS, and outdoor. Our model reaches an 87% PCK without fine-tuning on MPI-INF-3DHP.

3.5. Ablation Study

We explore the optimal design of the GCN block for the proposed architecture. As depicted in Fig. 3, we test the different designs of the GCN block which incorporate graph convolution into Transformer [10], ResNet [21], and ConvNeXt [22], respectively. The result and floating point operations (FLOPs)

are shown in Table 4. Our design is shown in Fig. 2. We found that a plain graph convolution followed by a graph convolution with the residual has the best result in our experiment.

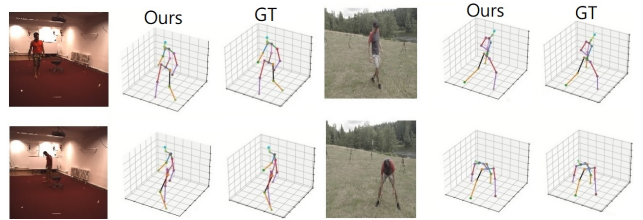


Fig. 4. Visualization on the test set of Human3.6M and MPI-INF-3DHP.

3.6. Qualitative Results

Fig. 4 shows some visualization results estimated by the proposed model on Human3.6M and MPI-INF-3DHP. AMPose correctly predicts 3D pose actors in various backgrounds. Even with the actors performing rare actions in outdoors can be accurately estimated by our model.

4. CONCLUSION

In this work, we have presented a novel architecture AMPose in which the Transformer encoder and GCN blocks are repeatedly stacked. In AMPose, the relations among joints are divided into two sets: the non-physical relations and physical connection in human joints, which can be modularized by the Transformer encoder and GCNs, respectively. The Transformer encoder is applied to connect each joint with all the other joints, while GCN is applied to capture the information of neighboring joints in the human body. The proposed method shows superior performance in accuracy and generalization ability by comparing with state-of-the-art models on Human3.6M and MPI-INF-3DHP datasets. However, the proposed model only takes accuracy performance as consideration. The lightweight model based on the proposed structure may be future work.

5. REFERENCES

- [1] Weixi Zhao, Weiqiang Wang, and Yunjie Tian, “Graformer: Graph-oriented transformer for 3d pose estimation,” in *2022 IEEE/CVF Conference on Computer Vision and Pattern Recognition (CVPR)*, 2022, pp. 20406–20415.
- [2] Dario Pavllo, Christoph Feichtenhofer, David Grangier, and Michael Auli, “3d human pose estimation in video with temporal convolutions and semi-supervised training,” in *Proceedings of the IEEE/CVF Conference on Computer Vision and Pattern Recognition (CVPR)*, 2019, pp. 7753–7762.
- [3] Yujun Cai, Liuhao Ge, Jun Liu, Jianfei Cai, Tat-Jen Cham, Junsong Yuan, and Nadia Magnenat Thalmann, “Exploiting spatial-temporal relationships for 3d pose estimation via graph convolutional networks,” in *2019 IEEE/CVF International Conference on Computer Vision (ICCV)*, 2019.
- [4] Wenhao Li, Hong Liu, Hao Tang, Pichao Wang, and Luc Van Gool, “Mhformer: Multi-hypothesis transformer for 3d human pose estimation,” in *Proceedings of the IEEE/CVF Conference on CVPR*, 2022.
- [5] Jinlu Zhang, Zhigang Tu, Jianyu Yang, Yujin Chen, and Junsong Yuan, “Mixste: Seq2seq mixed spatio-temporal encoder for 3d human pose estimation in video,” in *Proceedings of the IEEE/CVF Conference on CVPR*, 2022.
- [6] Tianhan Xu and Wataru Takano, “Graph stacked hourglass networks for 3d human pose estimation,” in *Proceedings of the IEEE/CVF conference on CVPR*, 2021.
- [7] Kenkun Liu, Rongqi Ding, Zhiming Zou, Le Wang, and Wei Tang, “A comprehensive study of weight sharing in graph networks for 3d human pose estimation,” in *European Conference on Computer Vision (ECCV)*, 2020.
- [8] Zhiming Zou and Wei Tang, “Modulated graph convolutional network for 3d human pose estimation,” in *2021 IEEE/CVF International Conference on Computer Vision (ICCV)*, 2021.
- [9] Thomas N Kipf and Max Welling, “Semi-supervised classification with graph convolutional networks,” *arXiv preprint arXiv:1609.02907*, 2016.
- [10] Ashish Vaswani, Noam Shazeer, Niki Parmar, Jakob Uszkoreit, Llion Jones, Aidan N Gomez, Łukasz Kaiser, and Illia Polosukhin, “Attention is all you need,” *Advances in neural information processing systems*, vol. 30, 2017.
- [11] Dan Hendrycks and Kevin Gimpel, “Gaussian error linear units (gelus),” *arXiv preprint arXiv:1606.08415*, 2016.
- [12] Hai Ci, Chunyu Wang, Xiaoxuan Ma, and Yizhou Wang, “Optimizing network structure for 3d human pose estimation,” in *2019 IEEE/CVF ICCV*, 2019.
- [13] Sebastian Lutz, Richard Blythman, Koustav Ghosal, Matthew Moynihan, Ciaran Simms, and Aljosa Smolic, “Jointformer: Single-frame lifting transformer with error prediction and refinement for 3d human pose estimation,” *arXiv preprint arXiv:2208.03704*, 2022.
- [14] Ailing Zeng, Xiao Sun, Fuyang Huang, Minhao Liu, Qiang Xu, and Stephen Lin, “Srnet: Improving generalization in 3d human pose estimation with a split-and-recombine approach,” in *ECCV*, 2020, pp. 507–523.
- [15] Michaël Defferrard, Xavier Bresson, and Pierre Vandergheynst, “Convolutional neural networks on graphs with fast localized spectral filtering,” *Advances in neural information processing systems*, vol. 29, 2016.
- [16] Long Zhao, Xi Peng, Yu Tian, Mubbasis Kapadia, and Dimitris N Metaxas, “Semantic graph convolutional networks for 3d human pose regression,” in *Proceedings of the IEEE/CVF conference on CVPR*, 2019, pp. 3425–3435.
- [17] Catalin Ionescu, Dragos Papava, Vlad Olaru, and Cristian Sminchisescu, “Human3. 6m: Large scale datasets and predictive methods for 3d human sensing in natural environments,” *IEEE transactions on pattern analysis and machine intelligence*, vol. 36, no. 7, pp. 1325–1339, 2013.
- [18] Dushyant Mehta, Helge Rhodin, Dan Casas, Pascal Fua, Oleksandr Sotnychenko, Weipeng Xu, and Christian Theobalt, “Monocular 3d human pose estimation in the wild using improved cnn supervision,” in *2017 international conference on 3D vision (3DV)*. IEEE, 2017, pp. 506–516.
- [19] Kun Zhou, Xiaoguang Han, Nianjuan Jiang, Kui Jia, and Jiangbo Lu, “Hemlets pose: Learning part-centric heatmap triplets for accurate 3d human pose estimation,” in *Proceedings of the IEEE/CVF ICCV*, 2019, pp. 2344–2353.
- [20] Yilun Chen, Zhicheng Wang, Yuxiang Peng, Zhiqiang Zhang, Gang Yu, and Jian Sun, “Cascaded pyramid network for multi-person pose estimation,” in *Proceedings of the IEEE conference on CVPR*, 2018.
- [21] Kaiming He, Xiangyu Zhang, Shaoqing Ren, and Jian Sun, “Deep residual learning for image recognition,” in *Proceedings of the IEEE conference on CVPR*, 2016.
- [22] Zhuang Liu, Hanzi Mao, Chao-Yuan Wu, Christoph Feichtenhofer, Trevor Darrell, and Saining Xie, “A convnet for the 2020s,” in *Proceedings of the IEEE/CVF Conference on CVPR*, 2022.